Available online at www.sciencedirect.com
SCIENCE DIRECT
Earth and Planetary Science Letters 244 (2006) 378–393
EPSL
www.elsevier.com/locate/epsl

Late Brunhes polarity excursions (Mono Lake, Laschamp, Iceland Basin and Pringle Falls) recorded at ODP Site 919 (Irminger Basin)

J.E.T. Channell *

Department Geological Sciences, POB 112120, University of Florida, Gainesville, FL 32611, USA

Received 2 October 2005; accepted 16 January 2006

Editor: V. Courtillot

Abstract

Component natural remanent magnetizations derived from u-channel and 1-cm^3 discrete samples from ODP Site 919 (Irminger Basin) indicate the existence of four intervals of negative inclinations in the upper Brunhes Chronozone. According to the age model based on planktic oxygen isotope data, these "excursional" intervals occur in sediments deposited during the following time intervals: 32–34 ka, 39–41 ka, 180–188 ka and 205–225 ka. These time intervals correspond to polarity excursions detected elsewhere, known as Mono Lake, Laschamp, Iceland Basin and Pringle Falls. The isotope-based age model is supported by the normalized remanence (paleointensity) record that can be correlated to other calibrated paleointensity records for the 0–500 ka interval, such as that from ODP Site 983. For the intervals associated with the Mono Lake and Laschamp excursions, virtual geomagnetic poles (VGPs) reach equatorial latitudes and mid-southerly latitudes, respectively. For intervals associated with the Iceland Basin and Pringle Falls excursions, repeated excursions of VGPs to high southerly latitudes indicate rapid directional swings rather than a single short-lived polarity reversal. The directional instability associated with polarity excursions is not often recorded, probably due to smoothing of the sedimentary record by the process of detrital remanence (DRM) acquisition.

Keywords: magnetic excursions; Brunhes Chron; Irminger Basin; paleointensity

1. Introduction

A taxonomic distinction between polarity excursions and polarity subchrons is appropriate in view of the likelihood that the two phenomena have distinct generation mechanisms related to the role of the inner core [1], and the observation that the duration of polarity reversals, as defined by the age range of transitional magnetization directions, often exceeds the duration of individual polarity excursions. We distinguish "polarity excursion (zone)" from "polarity subchron(ozone)" using a dividing duration of 30 kyr. Although the choice of duration limit (30 kyr) is fairly arbitrary, it is large enough to be resolvable through astrochronology and coincides with the duration limit between "cryptochrons" and "subchrons" in marine magnetic anomaly (MMA) data [2], and therefore coincides with the practical limit for recognition of polarity intervals in MMA data. Ten years ago, only five "excursions" were convincingly documented in the magnetostratigraphic records of the Brunhes Chron: (1) The Mono Lake Excursion at about 30 ka [3,4], (2) The Laschamp Excursion at about 40 ka [5–7], (3) The Blake

* Tel.: +1 352 392 3658; fax: +1 352 392 9294.
E-mail address: jetc@geology.ufl.edu.

0012-821X/$ - see front matter © 2006 Elsevier B.V. All rights reserved.
doi:10.1016/j.epsl.2006.01.021

Excursion at about 120 ka [8–11], (4) The Pringle Falls Excursion at about 220 ka [12,13] and (5) The Big Lost Excursion at ~565 ka [14,15].

In the last 10–15 yrs, one of the most important developments in magnetic stratigraphy has been the revelation of numerous polarity excursions within the Brunhes and Matuyama Chrons. Following Champion et al. [15] who made the case for 8 excursions within the Brunhes Chron, the number of excursions in the Brunhes Chron has proliferated to 12–15 [16–20] with little agreement as to their age or labeling (see Fig. 1 for 0–300 ka only). Lineated "tiny wiggles" in MMA data, included as 54 cryptochrons in the Cenozoic part of the timescale of Cande and Kent [2], may be attributed to either brief polarity excursions or paleointensity fluctuations [21]. Only one of these 54 cryptochrons lies in the Brunhes Chron (at 500 ka) and one in the Matuyama Chron (coincident with the so-called Cobb Mt. Subchron at 1.2 Ma) [2].

Valet and Meynadier [22] pointed out that lows in Brunhes paleointensity, in equatorial Pacific (ODP Leg 138) sediments, appear synchronized with directional excursions detected elsewhere. The sedimentation rates in Leg 138 sediments are, however, too low to record brief geomagnetic excursions, and therefore a direct correlation of excursions and paleointensity was not possible in these cores. The direct correlation of geomagnetic excursions to lows in relative paleointensity has since been achieved for the Laschamp Excursion [23–25] and for the Iceland Basin Excursion [26–29], and for some excursions in the Matuyama Chron [30–32]. Although the majority of proposed excursions have not been recorded within the sedimentary sections that have yielded paleointensity records, minima in paleointensity records have been labeled after coeval excursions recorded elsewhere (e.g. [33]).

The Norwegian–Greenland Sea and the Arctic Ocean/Yermak Plateau, close to Svalbard (Spitsbergen), has been fertile ground for magnetic excursions. Early records of the late Brunhes Chron from the Norwegian–Greenland Sea indicated several intervals of negative inclination [34], that have also been observed in piston cores from further north in the Fram Strait [35] and on the Yermak Plateau [36]. Lack of well-defined $\delta^{18}O$ records from these cores led to uncertainty in the age of the intervals of negative remanence inclination. Cores from the Greenland Basin, north of Jan Mayen Island, however, yielded negative remanence inclinations with $\delta^{18}O$ ages corresponding to the Mono Lake excursion (~27–28 ka), the Laschamp excursion (~40 ka), and an excursion at ~188 ka, referred to as the Biwa I/Jamaica excursion [37]. The label "Biwa 1/Jamaica" implies correlation of this excursion with excursions from early studies [38–40]. Nowaczyk and Kneis [41] found several excursions in cores from close to the Yermak Plateau, with age control from ^{14}C and $\delta^{18}O$, that were

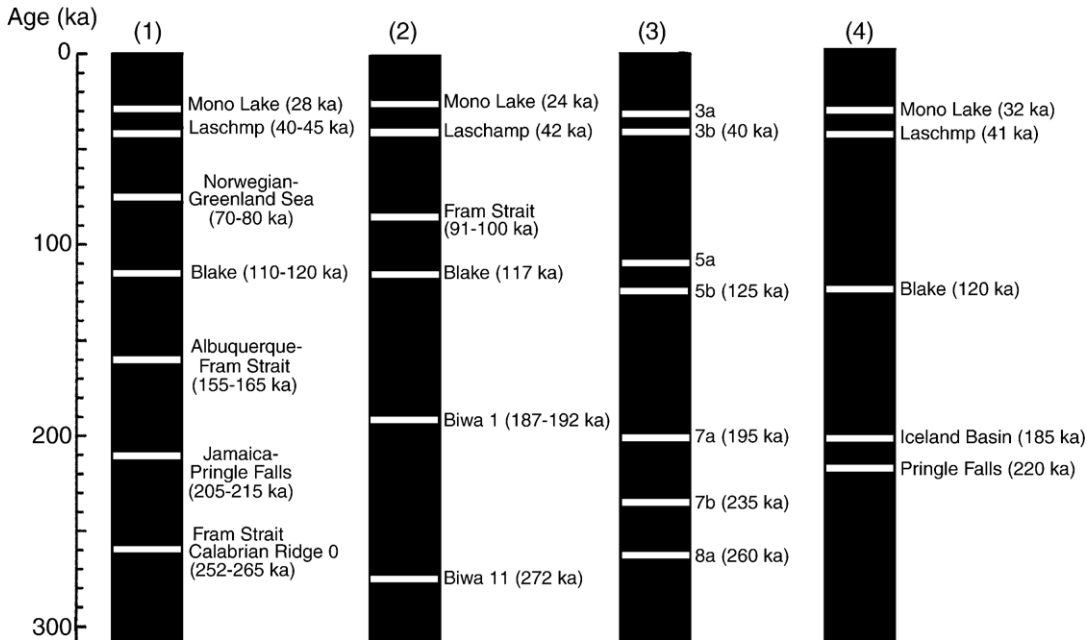

Fig. 1. Ages of geomagnetic excursions for the last 300 kyr according to different authors: Column 1: Langereis et al. [16], Column 2: Worm [17], Column 3: Lund et al. [19], Column 4: Selection of well-documented excursions with good age control (see text for references).

labeled: Mono Lake, Laschamp, Norwegian–Greenland Sea and Blake (see Fig. 1). One of the cores documented in this study (PS 2212-3 KAL) illustrates an anomaly common to these high latitude cores. The cumulative percentage thickness of reverse polarity zones in sediment accumulated during the last few 100 kyr is far greater than expected (~50% for the top 4 m of the section representing the last 120 kyr in PS2212-3KAL). Fortuitous fluctuations in sedimentation rates, not resolvable in the age models, appear to have "amplified" the excursional records.

Apart from its manifestation in the Norwegian–Greenland Sea and Arctic Ocean, the *Mono Lake excursion* has been recorded in detail at several locations in the Great Basin of western North America including the "type" section at Mono Lake [3,4,42]. The age of the Mono Lake excursion in its "type" area has been a recent topic of debate. Kent et al. [43] have made the case that the age uncertainty for the Mono Lake excursion is such that its age is indistinguishable from the age of the Laschamp Excursion (~40 ka). This argument has been countered by Benson et al. [44] who argue for an age close to 32 ka, about 8 kyr younger than the age attributed to the Laschamp Excursion. The inverse relationship between paleointensity and cosmogenic (^{36}Cl) flux in the GRIP (Greenland) ice core provides indirect evidence for paleointensity minima at ~30 ka and ~41 ka, coincident with the predicted age of the Mono Lake and Laschamp excursions [45]. Until a few years ago, records of the *Laschamp excursion* were restricted to volcanic records from France and Iceland [5–7]. The excursion has now been observed in sediment cores with robust age control dispersed over a large part of the North Atlantic and Gulf of Mexico [23,25,46], and in several cores from the South Atlantic and Indian oceans [24,46]. The *Blake excursion* has been recorded as a single reverse polarity zone [9], as two reverse zones [10,47,48] and as three reverse polarity zones [11,49]. The records have been derived from the Mediterranean, western Atlantic and Chinese loess. The excursion occurs in marine isotope stage (MIS) 5, probably in marine isotope substages 5e/5d [10]. The *Iceland Basin excursion* at ~188 ka observed in the Iceland Basin and Rockall Bank [29,50] is coeval with excursions recorded elsewhere in the North Atlantic [28,46,51] as well as in the Pacific [26,46,52] and South Atlantic oceans [53], and in Lake Baikal [54]. This excursion has been documented over a large portion of the globe, and can be correlated to the MIS 6/7 boundary. The *Pringle Falls excursion* was first documented in lacustrine sediments cropping out in Oregon near Pringle Falls [12,13] and Summer Lake [14], and subsequently at Long Valley, California [55]. Regional tephrochronology originally yielded age estimates close to 220 ka [13,55]. McWilliams [56] gave an ^{40}Ar/^{39}Ar age of 223±4 ka for this excursion based on ages from the Mamaku ignimbrites in New Zealand that carry excursional magnetization directions. Singer et al. [57] recently reported 16 laser incremental heating ages from plagioclase crystals derived from Ash D (deposited during the onset of the excursion at Pringle Falls) that define an ^{40}Ar/^{39}Ar isochron of 211 ka±13 ka. This age for the onset of the excursion at Pringle Falls brings the age of the excursion within ~20 kyr of the supposed age of the Iceland Basin Excursion at ~188 ka. Langereis et al. [16] considered the Pringle Falls excursion to be synonymous with the Jamaica excursion of Ryan and Flood [39] and gave an age estimate of 205–215 ka (Fig. 1).

2. ODP Site 919

ODP Site 919 (62.67°N, 37.46°W) is located in the Irminger Basin on the path of the East Greenland (surface) Current, and Denmark Strait overflow that forms a major component of North Atlantic Deep Water (NADW) (Fig. 2). The site is sensitive to millennial-scale instabilities of coastal ice sheets of the East Greenland/Icelandic area, and influenced by instabilities of the Laurentide Ice Sheet (Heinrich Events). The position of the site in the deeper part of the Irminger Basin at 2088 m water depth minimizes the influence of turbidites shedding off the Greenland continental slope [58].

Core SU90-24 (62.67°N, 37.37°W), located close to Site 919, is well documented but only 8.6 m long. AMS ^{14}C and planktic δ^{18}O indicate that its base has an age of ~59 ka [59] indicating a mean sedimentation rate of ~15 cm/kyr. Light planktic δ^{18}O and IRD (based on lithic counts) have been correlated to Heinrich events H1–H4, and the distinctive detrital carbonate signature of these events has been documented [60]. Magnetic susceptibility cycles mimic the Dansgaard/Oeschgar (D/O) temperature oscillations in the Greenland ice cores during MIS 3, and are a response to changes in deep water circulation [61]. The fidelity of the magnetite magnetization, and the absence of high coercivity remanence carriers has been established in SU90-24 by observation of rock magnetic characteristics [61], by the recognition of the Laschamp Excursion, and by the paleointensity record that can be correlated to other records in the region [23].

Two holes were drilled at Site 919 during ODP Leg 152 (Sept.–Nov. 1993). Hole 919A penetrated 93 mbsf

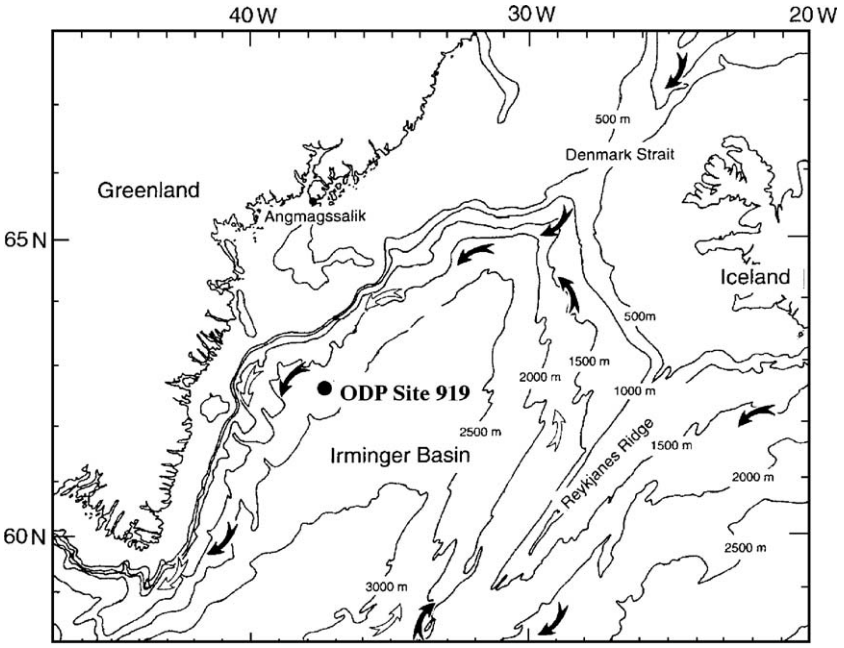

Fig. 2. Location of ODP Site 919 showing North Atlantic Deep Water (NADW) currents. Solid arrows indicate path of Denmark Strait Overflow Water (DSOW) and Iceland Scotland Overflow Water (ISOW), open arrows indicate path of Labrador Sea Water (LSW) (modified after [58]).

(meters below seafloor) and was then abandoned due to core barrel malfunction. Hole 919B was washed down from 18 mbsf to 90.0 mbsf, and coring was continued from 90 to 147 mbsf. At this depth, drilling was halted due to severe weather conditions. The recovery of gray silty clay and clayey silt was close to 100% at both holes [62]. Shipboard pass-through magnetometer data indicate that the Matuyama/Brunhes boundary lies at 122 mbsf [63] giving a mean Brunhes sedimentation rate of 15.6 cm/kyr. In the shipboard magnetic data, several intervals of low and negative remanence inclinations are apparent within the Brunhes Chronozone that may correspond to geomagnetic excursions, and it was these shipboard data that prompted this more detailed study.

At ODP Site 919, a planktic δ^{18}O record has been obtained from *N. pachyderma* (sin.) indicating that the base of the recovered section corresponds to MIS 25 [64]. This planktic δ^{18}O record has since been augmented by St. John et al. [65] who generated an age model based on the correlation of the Site 919 planktic record to the benthic δ^{18}O records from Core V19–30 and ODP Site 677 [66,67] as revised by Shackleton [68]. Here, we adopt the age model of St. John et al. [65] and compare their δ^{18}O record (placed on their age model) with the benthic composite δ^{18}O stack of Lisiecki and Raymo [69] from 57 globally distributed records (Fig. 3). The Site 919 planktic δ^{18}O record is strongly affected by meltwater that hinder a precise correlation to the benthic δ^{18}O (ice volume) record. The paucity of benthos precluded a benthic δ^{18}O record at this site. The younger part of the age model is supported by the presence of Ash Layer 2 at 11.19 mcd [65] corresponding to 56 ka (close to the generally adopted age of 55 ka for this prominent ash layer). The tie-points used to peg the age model, and the resulting mean sedimentation rates, are indicated in Fig. 4. Low sedimentation rates are associated with interglacial isotopic stages. Mean sedimentation rates appear to exceed 20 cm/kyr for MIS 3, and are generally enhanced for glacial stages (Fig. 4).

3. Sampling and methods

Continuous u-channel samples were collected from the archive half of Hole 919A. U-channel samples are enclosed in a plastic container that has the same length as the core section (usually 150 cm) and has a 2×2 cm square cross-section. One of the sides comprises a clip-on plastic lid that allows the sample to be sealed to inhibit dehydration and other chemical/physical changes. The meters composite depth (mcd) scale follows St. John et al. [65], and was based on splicing Holes 919A and 919B using the shipboard magnetic susceptibility record.

Natural remanent magnetization (NRM) of u-channel samples was measured at 1-cm spacing before

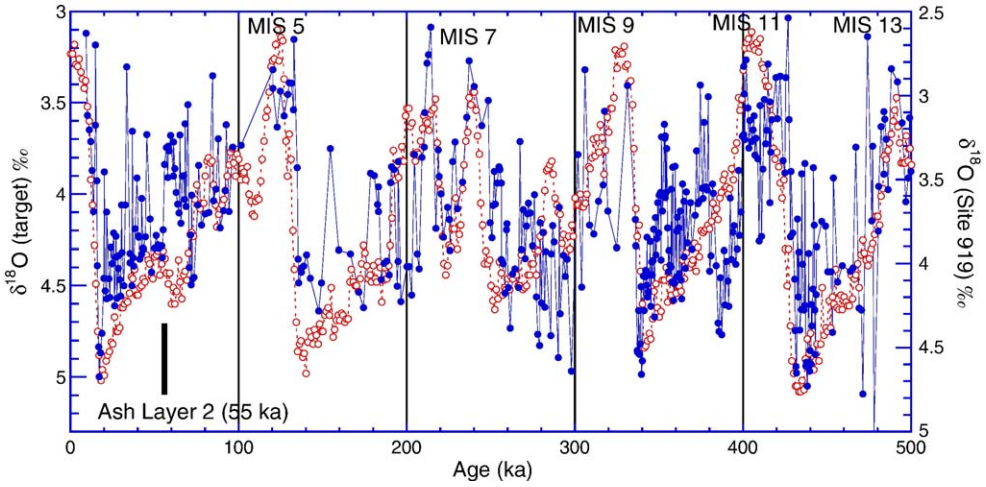

Fig. 3. ODP Site 919 planktic δ^{18}O record (closed symbols) from *N. pachyderma* (sin) [64,65] compared with the benthic δ^{18}O target (open symbols) [69].

demagnetization and at 14 demagnetization steps in the 10–100 mT peak field range, using a 2G Enterprises cryogenic magnetometer designed to measure u-channel samples. The response functions of the magnetometer pick-up coils have a width at half-height of ~4.5 cm [70], therefore, measurements at 1-cm spacing are not independent from one another. Deconvolution of the u-channel data [70,71] has been carried out on parts of the NRM record in order to improve the resolution of the measurements. Component magnetization directions were computed for all NRM data, as well as for deconvolved data, using the standard "principal component" method [72]. The demagnetization interval used to compute the characteristic magnetization component was generally 20–80 mT. The maximum angular deviation (MAD) values provide a means of monitoring the uncertainty associated with the component magnetization directions.

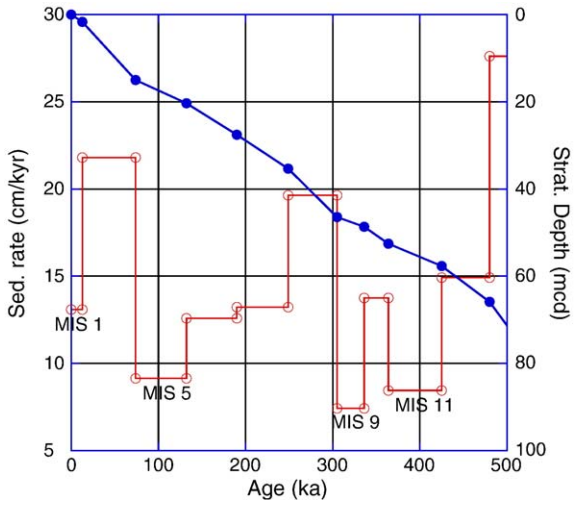

Fig. 4. Depth–age and sedimentation rates for ODP Site 919 according to the age model of St. John et al. [65].

Susceptibility measurements of u-channel samples were carried out using a susceptibility track with a pick-up loop that has a response function similar to that of the u-channel magnetometer used for remanence measurements [73]. Anhysteretic remanent magnetization (ARM) was acquired in a peak alternating field of 100 mT and a 50 nT DC bias field. ARM was measured prior to demagnetization and then after demagnetization at the same demagnetization steps used for NRM. Isothermal remanent magnetization (IRM) was acquired in a DC field of 500 mT, and was also demagnetized in the same steps applied to the NRM and ARM.

Back-to-back 1-cm^3 cubic discrete samples were collected alongside the u-channel trough across intervals where polarity excursions have been observed in the u-channel data. These discrete samples were demagnetized at 14 steps in the 10–100 mT peak field range and component magnetizations were then calculated using the standard method [72].

4. Magnetic properties and environmental magnetism

Magnetic concentration parameters, volume susceptibility and ARM intensity (Fig. 5), vary by less than an order of magnitude with a tendency for lower values during interglacial stages and glacial terminations. The parameter known as anhysteretic susceptibility (k_{arm}) is

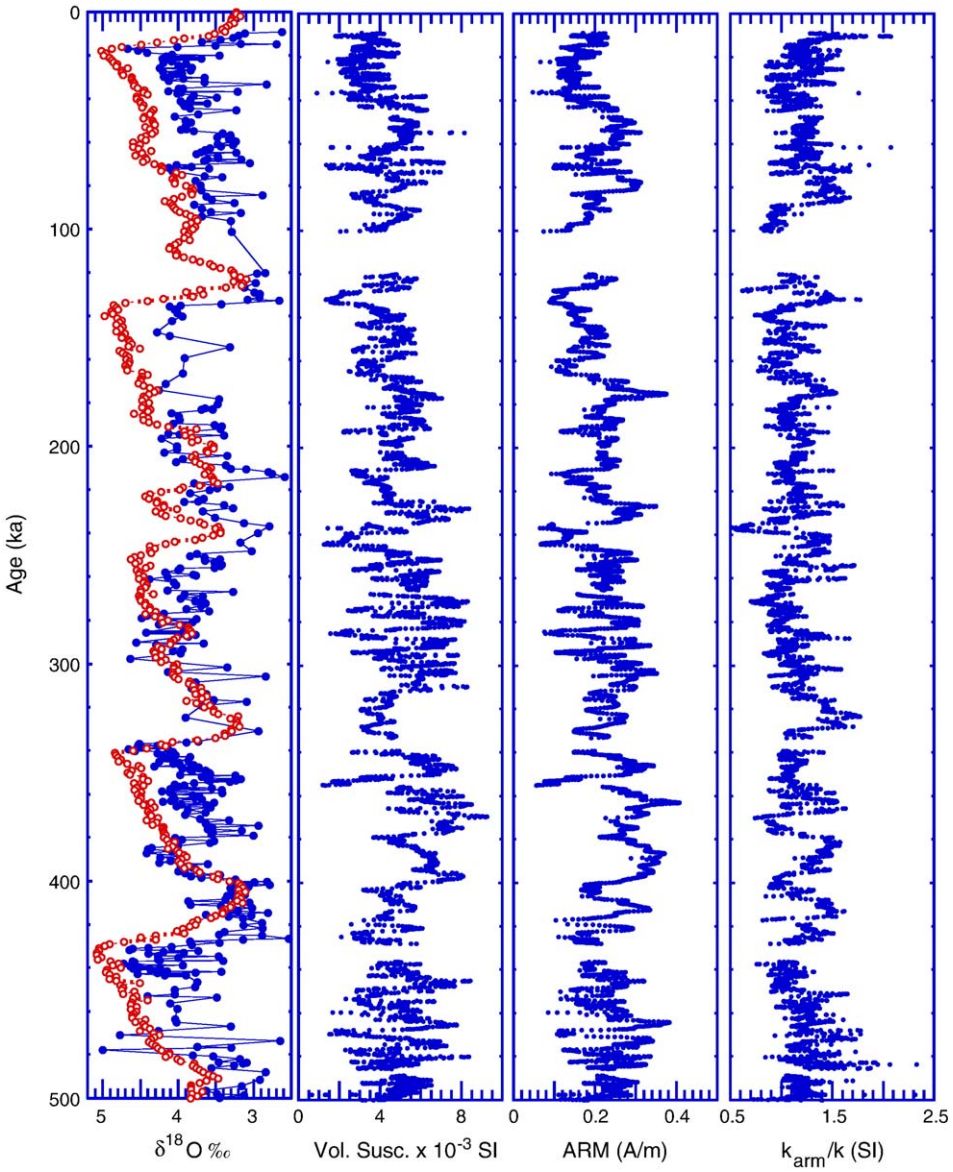

Fig. 5. ODP Site 919: planktic $\delta^{18}O$ record (closed symbols) [64,65] compared with the benthic $\delta^{18}O$ target (open symbols) [69] (as in Fig. 3) compared to volume susceptibility, ARM intensity after demagnetization at peak fields of 35 mT and the ratio of anhysteretic susceptibility to volume susceptibility (magnetite grain size proxy).

computed by normalizing $ARM_{35\ mT}$ by the DC bias field used to apply the ARM. The ratio k_{arm}/k, anhysteretic susceptibility divided by volume susceptibility (k), is often used as a grain-size proxy for magnetite (e.g. [74,75]). Higher values of the ratio imply finer magnetite grain sizes that occur preferentially during interglacial isotopic stages at Site 919 (Fig. 5). Following the calibration of k_{arm}/k by King et al. [74], the mean magnetite grain size at Site 919 is about 5 μm, and the grain size range appears to be restricted to a narrow (1–10 μm) range (Fig. 6).

For the last 100 kyr, for which Greenland ice-core $\delta^{18}O$ data are available [76,77], susceptibility at Site 919 appears to mimic the so-called "Dansgaard–Oeschger" (D–O) variability with low values of this and other magnetic concentration parameters coinciding with cold stadials (and hence Heinrich layers) in the ice core record (Fig. 7). We might expect the prominent interstadials (IS19–21) to correlate with highs in susceptibility, and the apparent mismatch in Fig. 7 may indicate either discrepancies in the Site 919 age model or a different relationship between magnetic

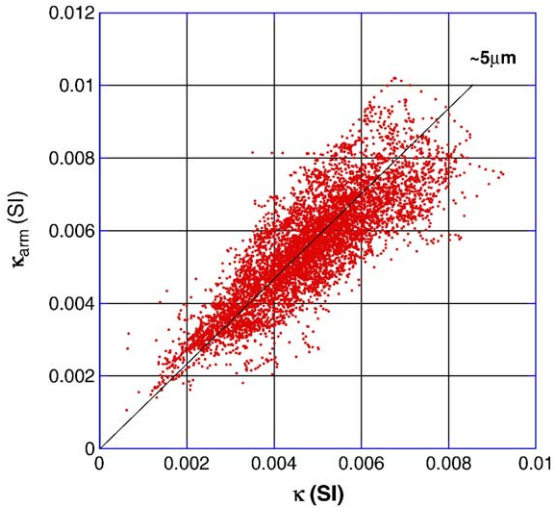

Fig. 6. ODP Site 919: Anhysteretic susceptibility (k_{arm}) plotted against susceptibility (k) indicative of a restricted magnetite grain-size range.

concentration parameters, such as susceptibility, and the temperature regime over Greenland during MIS 5 and MIS 3. As mentioned above, the observation of Ash Layer 2 at a level coinciding with the expected age (55 ka) anchors the age model in this part of the record. Susceptibility data from MIS 3 in Core SU90-24 [61], located close to Site 919, was used to correlate among North Atlantic cores, and variations were attributed to changes in bottom current activity that are apparently in phase with air temperature changes over Greenland as recorded by ice core $\delta^{18}O$ data. Note that the adopted Site 919 age model [65] has not been adjusted to improve the correlation of magnetic parameters to the ice core record, and the age model as it stands is not over-defined by a proliferation of age tie points (Fig. 4).

5. Natural remanent magnetization

Component declinations and inclinations (Fig. 8) were determined for u-channel samples by applying the standard method [72] each 1-cm down-core, utilizing demagnetization data in the 20–80 mT peak field range, with the origin of orthogonal projections not used in the computation. Maximum angular deviation (MAD) values are generally less than 5° indicating that the components are usually well defined. Higher MAD values are observed in the 30–40 ka and 180–220 ka

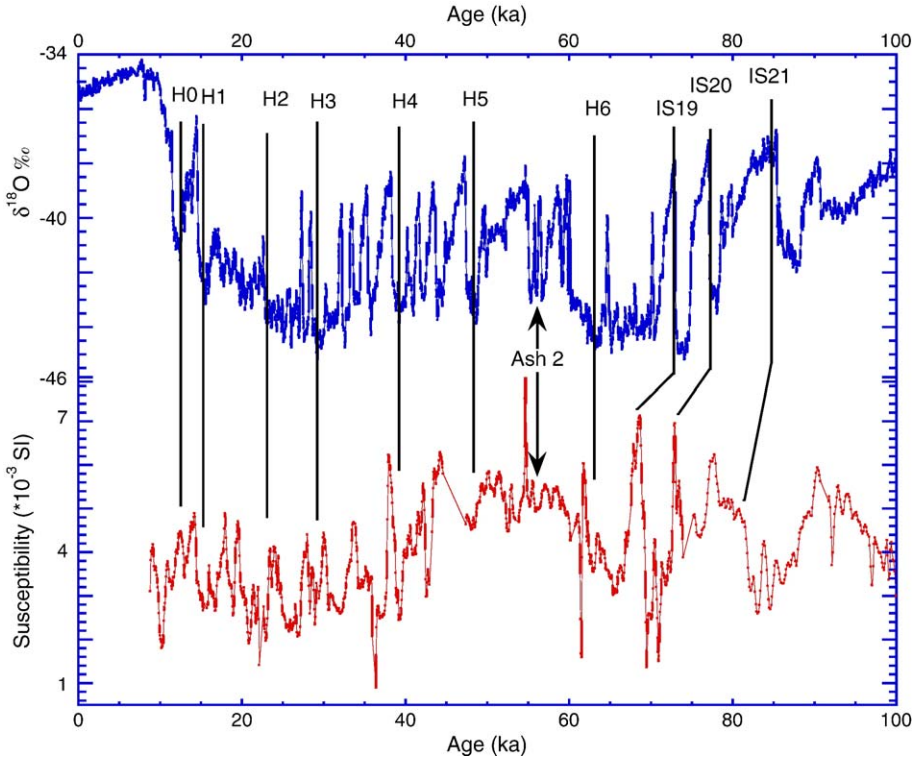

Fig. 7. Greenland ice-core $\delta^{18}O$ data [76,77] compared to ODP Site 919 susceptibility that appears to mimic the so-called "Dansgaard–Oeschger" (D–O) variability with relatively low values of magnetic susceptibility coinciding with cold stadials (and hence Heinrich layers, H0–H6) in the ice core record. The expected correlation of interstadials (IS) 19–21 to highs in the susceptibility record is offset possibly signifying discrepancies in the Site 919 age model. The location of Ash Layer 2 anchors the age model at ~55 ka.

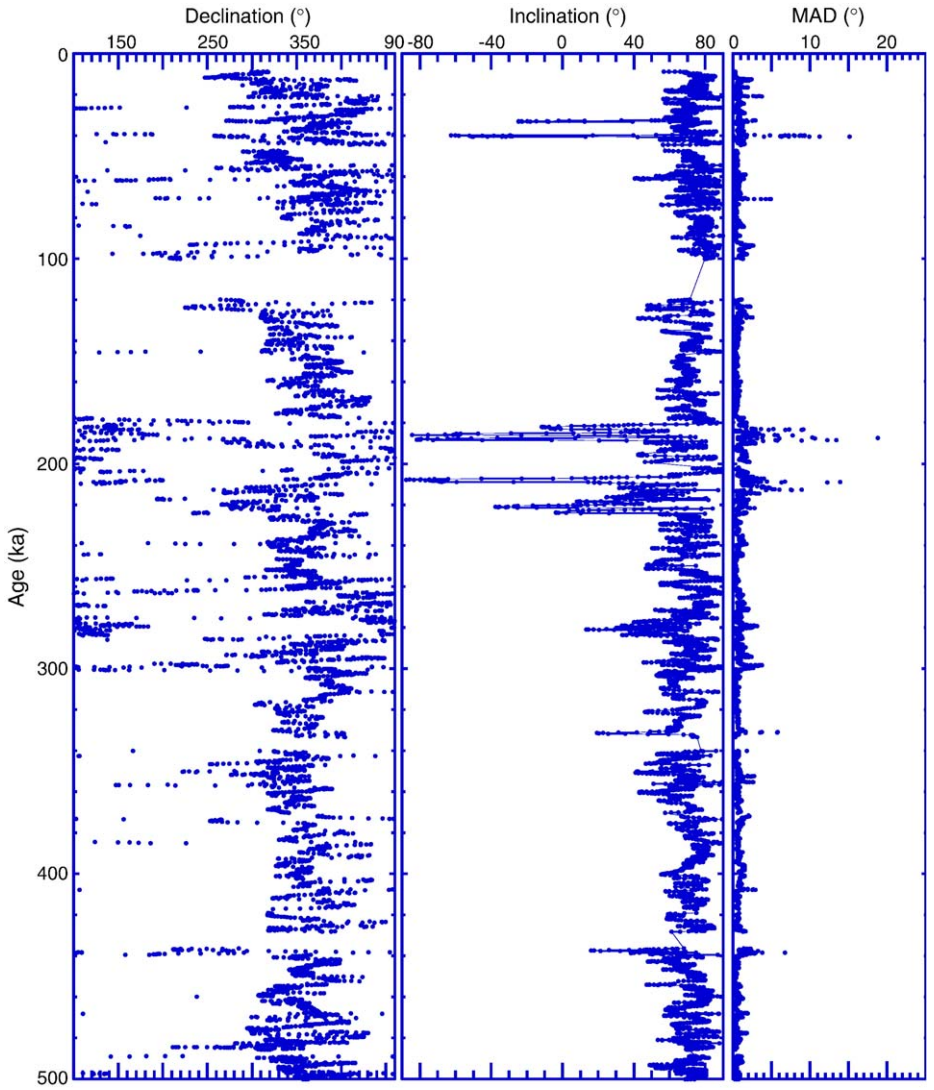

Fig. 8. ODP Site 919: Component declination and inclination and accompanying maximum angular deviation (MAD) values from u-channel data computed for the 20–80 mT demagnetization interval (without anchoring to the origin of orthogonal projections), and for each 1-cm down-core.

intervals (Fig. 8) reflecting more complex magnetizations, including abrupt changes in magnetization directions and/or superimposition of magnetization components, in these two intervals recording polarity excursions. In these two intervals, we collected 1-cm^3 discrete samples, back-to-back alongside the u-channel trough. The NRM of these discrete samples was stepwise demagnetized in order to compare the discrete sample data with the u-channel data, and with the u-channel data after deconvolution. The u-channel data are smoothed by the shape of the response function and possibly perturbed by end-effects and interference between orthogonal magnetometer pick-up coils. Deconvolution is designed to mitigate these problems although deconvolution introduces (other) additional noise. Discrete samples, particularly 1-cm^3 discrete samples, are affected by deformation of sediment close to the walls of the sample container. The MAD values computed for u-channel data, deconvolved u-channel data (deconvolution is carried out for each demagnetization step), and discrete samples, give a measure of the uncertainty in component magnetization directions for each dataset (Fig. 9).

Orthogonal projections of u-channel, deconvolved u-channel data, and 1-cm^3 discrete samples are compared for five depths (ages) corresponding to intervals of negative inclination components (Fig. 10). Magnetizations directions derived from u-channels occasionally

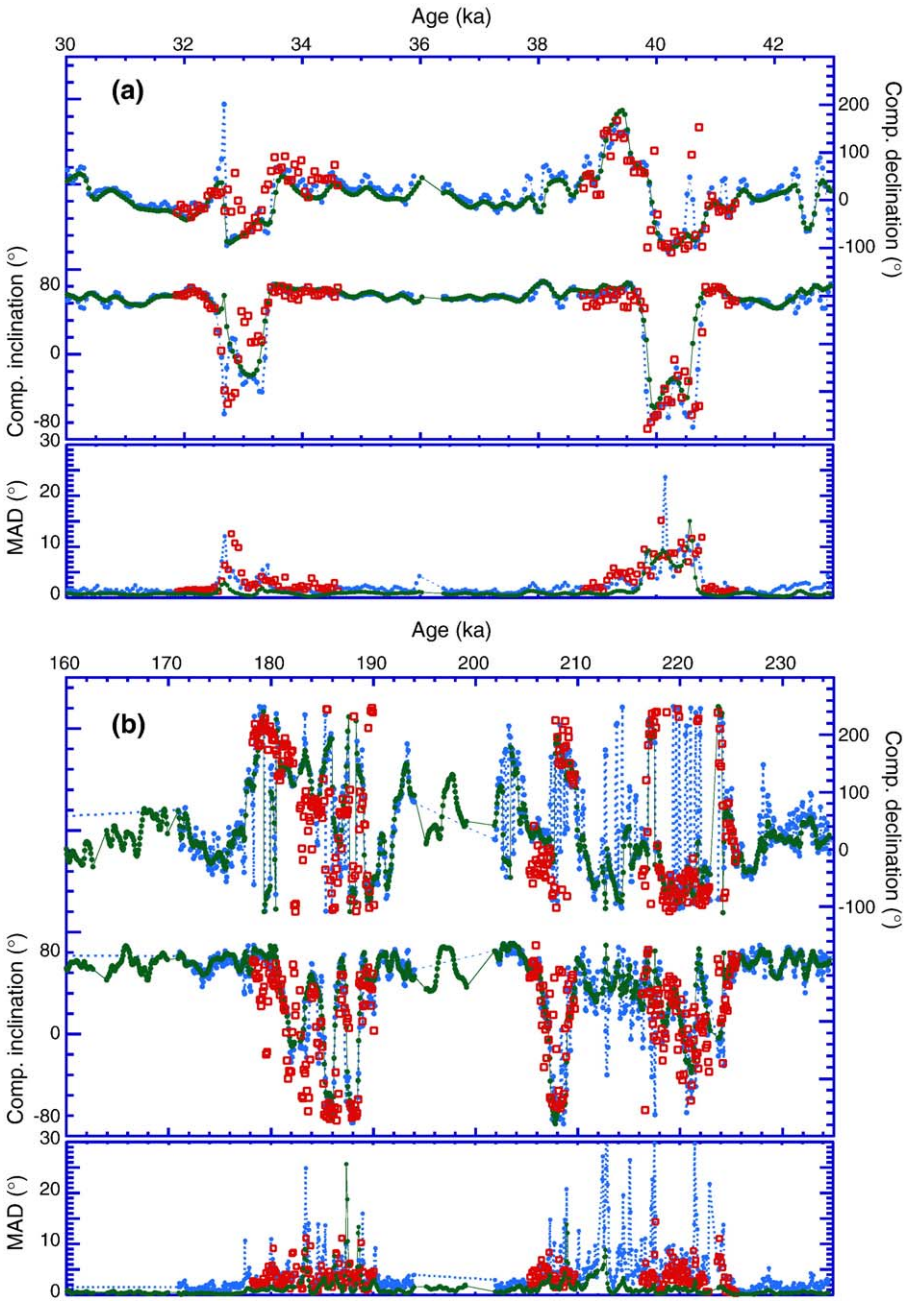

Fig. 9. ODP Site 919: Component declination and inclination, and accompanying maximum angular deviation (MAD) values, for u-channel data (dark/green closed symbols connected by line), deconvolved u-channel data (closed gray/blue symbols connected by dashed line) and data from 1-cm^3 discrete samples (open/red squares without connecting line).

differ substantially before and after deconvolution (see Laschamp and Pringle Falls II in Fig. 10), particularly in intervals of rapid directional change as would be expected. Discrete sample directions occasionally differ from u-channel directions (see Iceland Basin in Fig. 10). These differences may be attributed to smoothing in the u-channel data due to the magnetometer response function, sediment deformation associated with 1-cm^3 discrete sampling, or imprecise mm-scale depth correlation of u-channels and discrete samples, exacerbated by the fact that these two sample types were collected during separate visits to the core repository. We note that the deconvolved u-channel data displayed in Fig. 9 are generally more consistent with the 1-cm^3 discrete

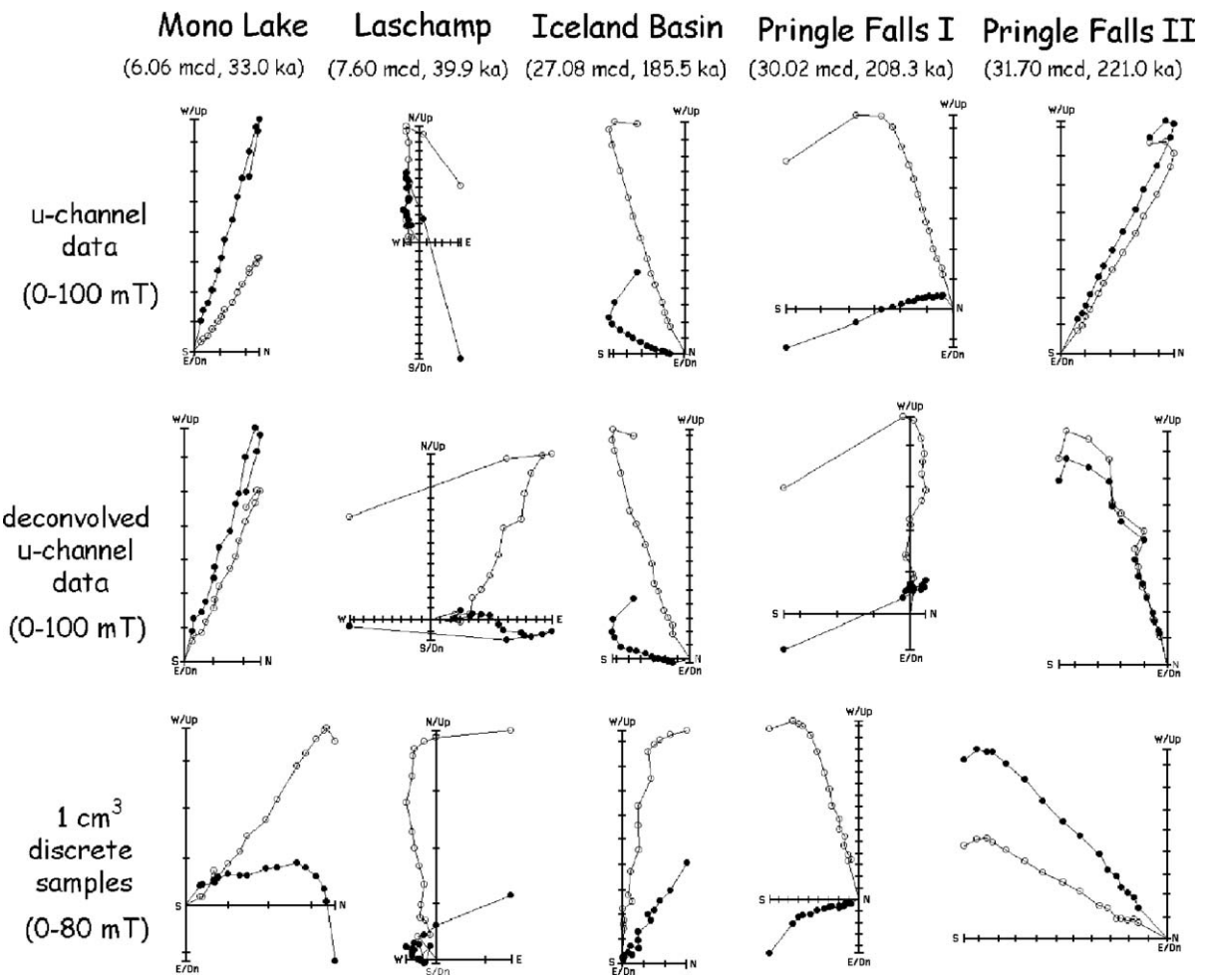

Fig. 10. Orthogonal projections of demagnetization data for representative samples from five intervals of ODP Site 919 displaying negative inclinations for three data-types from the same depth (age): u-channel data (without deconvolution), u-channel data with deconvolution, and discrete (1-cm^3) samples. Open (closed) symbols represent vector end points projected on the vertical (horizontal) plane, respectively. (one division on the intensity scales corresponds to 0.01 A/m).

sample data than with the u-channel data prior to deconvolution. For the 205–225 ka interval, the deconvolved u-channel data are particularly erratic and associated with MAD values >10° (Fig. 9), possibly due to "noise" introduced into the deconvolved data by abrupt changes in magnetization direction.

It has already been demonstrated by susceptibility and ARM data that the magnetite grain size is restricted to a narrow range throughout the section (Fig. 6). In order to monitor magnetic mineralogy and magnetite grain size changes in the vicinity of the directional excursions, including the transitions in and out of the excursions, we measured magnetic hysteresis parameters on 82 samples using a Princeton Measurements Corp. (Model 3900) vibrating sample magnetometer (VSM). Samples were collected at about 2-cm spacing across intervals characterized by negative or low inclinations. For all measured samples, saturation magnetization was acquired in 200–300 mT applied fields, and hysteresis ratios are tightly grouped in the pseudo-single domain (PSD) field in the Day plot [78] (Fig. 11), precluding the possibility that changes in magnetization direction are lithologically controlled. Table 1 (EPSL Background Dataset) gives the depth (mcd) and age and the hysteresis parameters for each interval: Mono Lake interval (20 samples), Laschamp interval (8 samples), Iceland Basin interval (29 samples) and Pringle Falls interval (25 samples).

6. Paleointensity proxies

Concentration parameters such as susceptibility (k) and $ARM_{35\ mT}$ vary by less than an order of magnitude (Fig. 5) and, together with the grain size uniformity

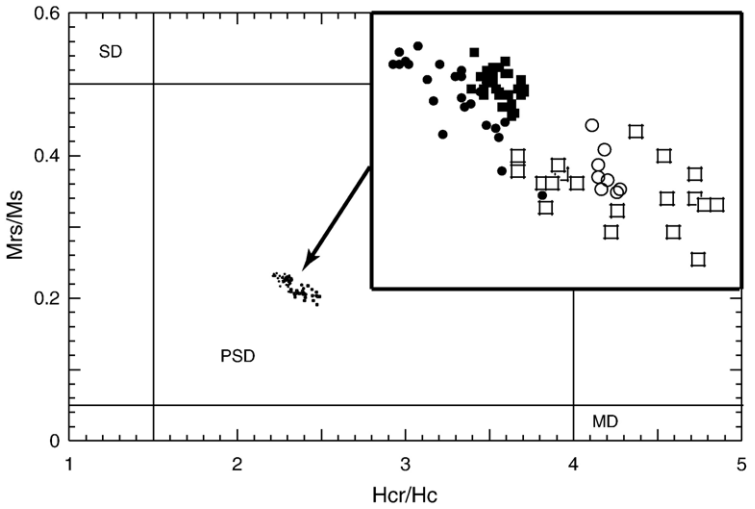

Fig. 11. Plot of hysteresis ratios with single domain (SD), pseudo-single domain (PSD) and multidomain (MD) fields for magnetite after [78]. Samples collected at ~2 cm intervals across intervals characterized by negative or low inclinations associated with the Mono Lake excursion (open squares), the Laschamp excursion (open circles), the Iceland Basin excursion (closed squares) and the Pringle Falls excursion (closed circles). Table 1 (EPSL Background Dataset) gives the depth (mcd), age, and hysteresis parameters for each interval: Mono Lake interval (20 samples), Laschamp interval (8 samples), Iceland Basin interval (29 samples) and Pringle Falls interval (25 samples).

(Figs. 6 and 11), these characteristics bode well for the determination of paleointensity proxies, that are only likely to be useful if the magnetite concentration and grain size are restricted to a narrow range (see [75]). The paleointensity proxies are calculated as the mean of NRM/ARM and the mean of NRM/IRM, both calculated over the 30–70 mT demagnetization range. The pattern of variability for the two Site 919 paleointensity proxies (Fig. 12a) is similar although mean NRM/IRM values are more variable than mean NRM/ARM values, with extreme high and low values. The standard deviation of the mean is generally greater for mean NRM/IRM than for NRM/ARM. Comparison of the NRM/ARM paleointensity proxy with the calibrated paleointensity record from northern Gardar Drift at ODP Site 983 [27,29] and with the Sint-800 paleointensity stack [79] supports the Site 919 age model and indicates that the Site 919 paleointensity pattern is quite typical, at least for the North Atlantic (Fig. 12b). Discrepancies in the match of paleointensity records between Site 919 and Site 983 in the 250–350 ka interval may indicate problems in the Site 919 age model in MIS 8–9 interval where the planktic oxygen isotope record is a poor match to the target curve (Fig. 3). The Sint-800 paleointensity stack [79] is highly smoothed relative to the records from ODP Sites 983 and 919, because the Sint-800 stack was derived from a stack of records with relatively low sedimentation rates. Table 2 (EPSL Background Dataset) provides the Site 919 mean NRM/ARM dataset as a function of age.

7. Conclusions

The excursional NRM directions at Site 919 occur during intervals of low relative paleointensity centered on 34 ka and 40 ka, and in the extended period of low paleointensity in the 180–225 ka interval (Fig. 12). Assuming that the ODP Site 919 age model is reliable, the excursion at 34 ka coincides with the so-called Mono Lake excursion of the same age recorded at several locations in the Great Basin of western North America including the "type" section at Mono Lake [3,4,42]. The age of the Mono Lake excursion in California is controversial. The age uncertainty makes it problematic to differentiate it from the age of the Laschamp excursion at ~40 ka [43]. Adding to the uncertainty, the Mono Lake excursion has not (until now) been unequivocally recorded outside the western USA. On the other hand, two maxima in flux of ^{36}Cl in Greenland ice [45], implying minima in geomagnetic field strength, and coincident with dual minima in marine relative paleointensity records (e.g. [23]) are consistent with a directional excursion about 6 kyr younger than the Laschamp excursion. The Laschamp excursion is now well established and has been firmly correlated to isotopic and ice-core age models [23–25,46] at 40–41 ka. The older of the two excursions featured in Fig. 9a is correlated to the Laschamp excursion.

The Iceland Basin excursion is correlated to the MIS 6/7 boundary and has been dated at 186–189 ka, with a

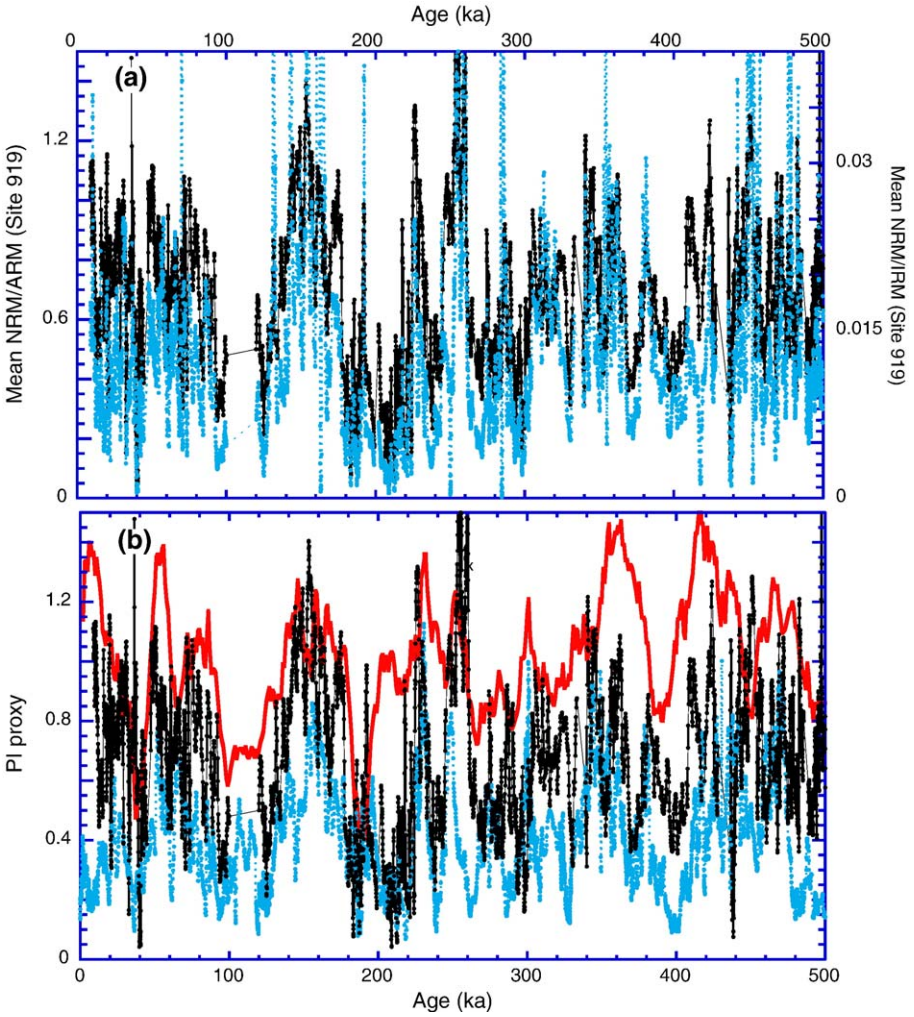

Fig. 12. (a) Site 919: Mean NRM/ARM (black points joined by continuous line) compared to mean NRM/IRM (gray/blue points joined by gray dashed line). (b) Site 919 mean NRM/ARM (black points joined by continuous line) compared with the paleointensity proxy (NRM/IRM) from ODP Site 983 [27,29] (gray/blue points joined by gray dashed line) and with the Sint-800 paleointensity stack [79] (thick red line without points).

estimated duration of 3 kyr [29]. The excursion has been detected in the North Atlantic [27–29,46], South Atlantic [53] and Pacific [26,46] oceans, and in Lake Baikal [54]. The younger of the two excursions featured in Fig. 9b is believed to be the Iceland Basin excursion. The u-channel data, the deconvolved u-channel data, and the 1-cm^3 discrete sample, all indicate that this record of the Iceland Basin excursion is more complex than other records of the same excursion, with several swings in inclination from high positive to high negative values. The onset of the excursional directions at 188 ka and the cessation of the excursional directions at 180 ka yields a duration of 8 kyr according to the (imperfect) Site 919 age model.

At 209–207 ka (Fig. 9b), there is an excursion to high negative inclinations, with an interval of apparent instability of the geomagnetic field preceding it that extends back to 225 ka. We tentatively associate this excursion, and the instability that precedes it, with the Pringle Falls excursion. As explained above, the Pringle Falls excursion has been recorded in California and Oregon [12–14,55] and its onset has been assigned an age of ~211 ka [57]. Langereis et al. [16] considered the Pringle Falls excursion to be synonymous with the Jamaica excursion of Ryan and Flood [39] and gave an age estimate for this excursion of 205–215 ka.

In Fig. 13, we use virtual geomagnetic polar (VGP) plots as a means of displaying component magnetization directions, without implying that excursional

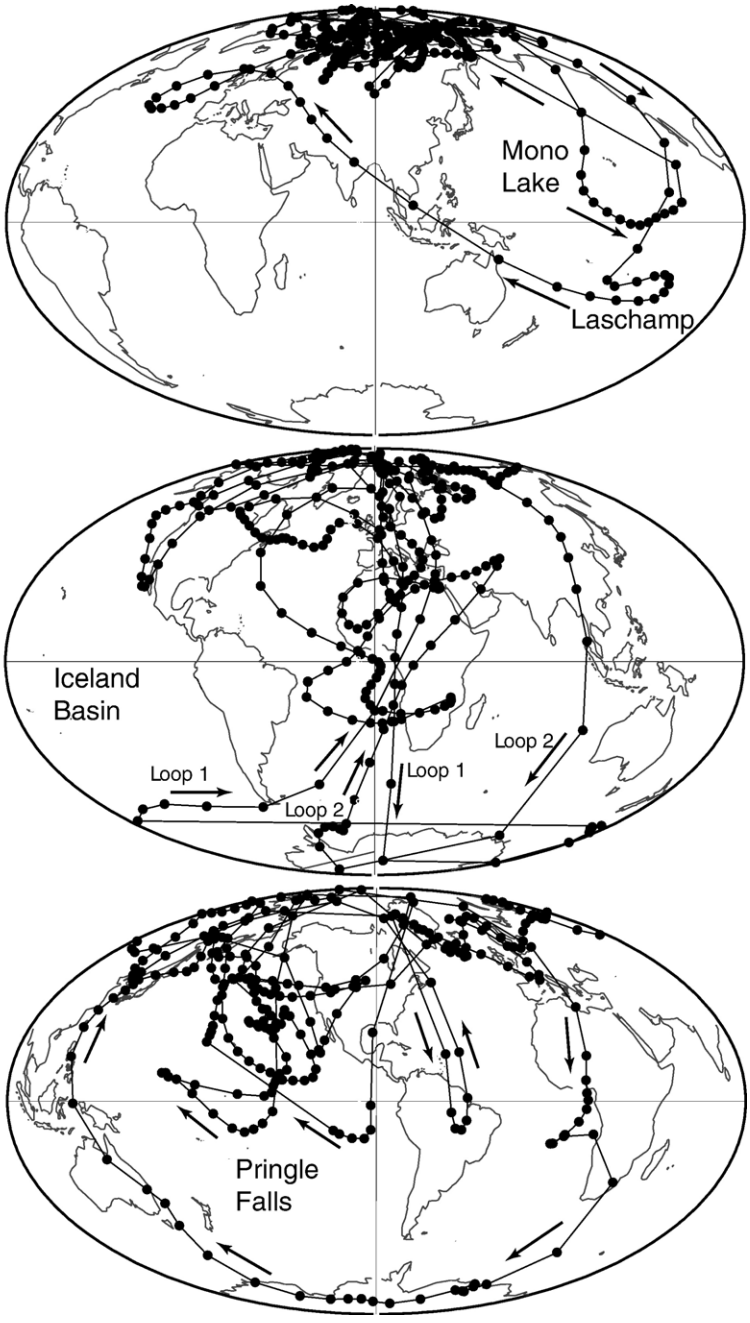

Fig. 13. Virtual geomagnetic poles (VGPs) for u-channel data, spaced at 1-cm, from the Mono Lake and Laschamp interval (30–43 ka), from the Iceland Basin interval (171–194 ka) and from the Pringle Falls interval (201–245 ka). Corresponding declination and inclination data are displayed in Fig. 9.

geomagnetic fields were necessarily dipolar. VGPs for the excursion recorded in the 39–41 ka interval at Site 919 (Fig. 9a), interpreted as the Laschamp excursion, describe a clockwise loop over the Pacific and SE Asia (Fig. 13). A clockwise VGP loop, centered on the Indian Ocean, has been found for the Laschamp excursion from widely dispersed sites (see [23,25,46]). The subsequent anticlockwise VGP loop, also over the Pacific (Fig. 13), corresponds to the excursion recorded at 32–34 ka (Fig. 9a) coeval with the Mono Lake excursion.

The excursion recorded in the 180–188 ka interval at Site 919 (Fig. 9b) is interpreted as the Iceland Basin

excursion. The VGP path for the 171–194 ka interval features two loops to high southerly latitudes (Loop 1 and Loop 2 in Fig. 13) followed by a complex group of VGPs at low latitudes over western Africa. This pattern of clockwise loops is different from the anticlockwise loops for this excursion found by others [29,46].

The excursion recorded in the 205–225 ka interval at Site 919 (Fig. 9b) describes a complex series of loops over the Pacific, South America and Africa, followed by a clockwise loop to high southerly latitudes (labeled Pringle Falls in Fig. 13). The final VGP loop is not dissimilar to the VGP loop recorded at the type section for the Pringle Falls excursion [13] and in the excursion recorded at ODP Sites 883 and 884 in the North Pacific [26,46]. We interpret the excursion recorded in the 205–225 ka interval at Site 919 as the Pringle Falls excursion.

We conclude that directional instability is a characteristic of the geomagnetic field at times of polarity excursions. Polarity excursions are observed at time of low paleointensity (Fig. 12) when the strength of the axial dipole is reduced by a factor of about 5, and reduced relative to the non-axial dipole (NAD) field. Zhang and Gubbins [80] have shown that the critical Reynolds number (R_c) for the onset of core convection is very sensitive to the poloidal field, and the strength of core convection varies wildly in response changes in magnetic field strength particularly during intensity minima. Geomagnetic field instability with rapid changes in magnetization directions is to be expected at times of low geomagnetic field intensity. Depositional and diagenetic processes always influence, to a greater or lesser extent, sedimentary records of excursions, however, the continuity of sedimentary records usually gives them a clear advantage over the inevitably discontinuous records from volcanic rocks. Although some sedimentary records of excursions indicate repetition of excursional directional features [11,13,25,54], as observed at ODP Site 919, all excursional records in sediments are, to a greater or lesser extent, smoothed and hence perturbed by the remanence acquisition process.

Acknowledgements

I thank Kristen St. John and Ben Flower for discussions concerning the age model at ODP Site 919, Kainian Huang and Helen Evans for help in the laboratory, and the ODP curatorial staff in College Station and Bremen for facilitating sample collection. The US National Science Foundation supported this research through grant OCE-0350830.

Appendix A. Supplementary data

Supplementary data associated with this article can be found, in the online version, at doi:10.1016/j.epsl.2006.01.021.

References

[1] D. Gubbins, The distinction between geomagnetic excursions and reversals, Geophys. J. Int. 137 (1999) F1–F3.
[2] S.C. Cande, D.V. Kent, A new geomagnetic polarity timescale for the late Cretaceous and Cenozoic, J. Geophys. Res. 97 (1992) 13917–13951.
[3] J.C. Liddicoat, R.S. Coe, Mono Lake geomagnetic excursion, J. Geophys. Res. 84 (1979) 261–271.
[4] R.M. Negrini, J.O. Davis, K.L. Verosub, Mono Lake geomagnetic excursion found at Summer Lake, Oregon, Geology 12 (1984) 643–646.
[5] N. Bonhommet, J. Babkine, Sur la presence d'aimentation inverse dans la Chaine des Puys, C. R. Hebd. Seances Acad. Sci., Ser. B 264 (1967) 92–94.
[6] N. Bonhommet, J. Zahringer, Paleomagnetism and potassium argon determinations of the Laschamp geomagnetic polarity event, Earth Planet. Sci. Lett. 6 (1969) 43–46.
[7] S. Levi, H. Gudmunsson, R.A. Duncan, L. Kristjansson, P.V. Gillot, S.P. Jacobsson, Late Pleistocene geomagnetic excursion in Icelandic lavas: confirmation of the Laschamp excursion, Earth Planet. Sci. Lett. 96 (1990) 443–457.
[8] J.D. Smith, J.H. Foster, Geomagnetic reversal in the Brunhes normal polarity epoch, Science 163 (1969) 565–567.
[9] P. Tucholka, M. Fontugue, F. Guichard, M. Paterne, The Blake polarity episode in cores from the Mediterranean Sea, Earth Planet. Sci. Lett. 86 (1987) 320–326.
[10] E. Tric, C. Laj, J.-P. Valet, P. Tucholka, M. Paterne, F. Gichard, The Blake geomagnetic event: transition geometry, dynamical characteristics and geomagnetic significance, Earth Planet. Sci. Lett. 102 (1991) 1–13.
[11] R.X. Zhu, L.P. Zhou, C. Laj, A. Mazaud, D.L. Ding, The Blake geomagnetic polarity episode recorded in Chinese loess, Geophys. Res. Lett. 21 (1994) 697–700.
[12] E. Herrero-Bervera, C.E. Helsley, S.R. Hammond, L.A. Chitwood, A possible lacustrine paleomagnetic record of the Blake episode from Pringle Falls, Oregon, USA, Phys. Earth Planet. Int. 56 (1989) 112–123.
[13] E. Herrero-Bervera, C.E. Helsley, A.M. Sarna-Wojcicki, K.R. Lajoie, C.E. Meyer, M.O. McWilliams, R.M. Negrini, B.D. Turrin, J.M. Donnelly-Nolan, J.C. Liddicoat, Age and correlation of a paleomagnetic episode in the western United States by $^{40}Ar/^{39}Ar$ dating and tephrochronology: the JAMAica, Blake, or a new polarity episode? J. Geophys. Res. 99 (1994) 24,091–24,103.
[14] R.M. Negrini, K.L. Verosub, J.O. Davis, Long-term non-geocentric axial dipole directions and a geomagnetic excursion from the middle Pleistocene sediments of the Humbolt River canyon, Pershing County, Nevada, J. Geophys. Res. 92 (1987) 10,617–10,627.
[15] D.E. Champion, M.A. Lanphere, M.A. Kuntz, Evidence for a new geomagnetic reversal from lava flows in Idaho: discussion of short polarity reversals in the Brunhes and late Matuyama Chrons, J. Geophys. Res. 93 (1988) 11,667–11,680.

[16] C.G. Langereis, M.J. Dekkers, G.J. de Lange, M. Paterne, P.J.M. van Santvoort, Magnetostratigraphy and astronomical calibration of the last 1.1 Myr from an eastern Mediterranean piston core and dating of short events in the Brunhes, Geophys. J. Int. 129 (1997) 75–94.
[17] H.-U. Worm, A link between geomagnetic reversals and events and glaciations, Earth Planet. Sci. Lett. 147 (1997) 55–67.
[18] S.P. Lund, G. Acton, B. Clement, M. Hastedt, M. Okada, T. Williams, ODP Leg 172 Scientific Party, Geomagnetic field excursions occurred often during the last million years, Trans. Am. Geophys. Union (EOS) 79 (14) (1998) 178–179.
[19] S.P. Lund, G.D. Acton, B. Clement, M. Okada, T. Williams, Brunhes Chron magnetic field excursions recovered from Leg 172 sediments, in: L.D. Keigwin, D. Rio, G.D. Acton, E. Arnold (Eds.), Proc. ODP, Sci. Results, vol. 172, 2001, pp. 1–18, Online.
[20] S.P. Lund, G.D. Acton, B. Clement, M. Okada, T. Williams, Paleomagnetic records of Stage 3 excursions, Leg 172, in: L.D. Keigwin, D. Rio, G.D. Acton, E. Arnold (Eds.), Proc. ODP, Sci. Results, vol. 172, 2001, pp. 1–20, Online.
[21] S.C. Cande, D.V. Kent, Ultrahigh resolution marine magnetic anomaly profiles: a record of continuous paleointensity variations? J. Geophys. Res. 97 (1992) 15,075–15,083.
[22] J.-P. Valet, L. Meynadier, Geomagnetic field intensity and reversals during the last four million years, Nature 366 (1993) 234–238.
[23] C. Laj, C. Kissel, A. Mazaud, J.E.T. Channell, J. Beer, North Atlantic PaleoIntensity Stack since 75ka (NAPIS-75) and the duration of the Laschamp Event, Philos. Trans. R. Soc., Ser. A (2000) 1009–1025.
[24] J.E.T. Channell, J.S. Stoner, D.A. Hodell, C. Charles, Geomagnetic paleointensity for the last 100 kyr from the subantarctic South Atlantic: a tool for interhemispheric correlation, Earth Planet. Sci. Lett. 175 (2000) 145–160.
[25] S.P. Lund, M. Schwartz, L. Keigwin, T. Johnson, Deep-sea sediment records of the Laschamp geomagnetic field excursion (~41,000 calendar years before present), J. Geophys. Res. 110 (2005) B04101, doi:10.1029/2003JB002943.
[26] A.P. Roberts, B. Lehman, R.J. Weeks, K.L. Verosub, C. Laj, Relative paleointensity of the geomagnetic field over the last 200,000 years from ODP Sites 883 and 884, North Pacific Ocean, Earth Planet. Sci. Lett. 152 (1997) 11–23.
[27] J.E.T. Channell, D.A. Hodell, B. Lehman, Relative paleointensity $\delta^{18}O$ at ODP Site 983, since 350 ka, Earth Planet. Sci. Lett. 153 (1997) 103–118.
[28] B. Lehman, C. Laj, C. Kissel, A. Mazaud, M. Paterne, L. Labeyrie, Relative changes of the geomagnetic field intensity during the last 280 kyear from piston cores in the Azores area, Phys. Earth Planet. Int. 93 (1996) 269–284.
[29] J.E.T. Channell, Geomagnetic paleointensity and directional secular variation at Ocean Drilling Program (ODP) Site 984 (Bjorn Drift) since 500 ka: comparisons with ODP Site 983 (Gardar Drift), J. Geophys. Res. 104 (1999) 22,937–22,951.
[30] Y. Guyodo, C. Richter, J.-P. Valet, Paleointensity record from Pleistocene sediments (1.4–0 Ma) off the California Margin, J. Geophys. Res. 104 (1999) 22,953–22,964.
[31] J.E.T. Channell, A. Mazaud, P. Sullivan, S. Turner, M.E. Raymo, Geomagnetic excursions and paleointensities in the 0.9–2.15 Ma interval of the Matuyama Chron at ODP Site 983 and 984 (Iceland Basin), J. Geophys. Res. 107 (B6) (2002), doi:10.1029/2001JB000491.
[32] C.S. Horng, A.P. Roberts, W.T. Liang, Astronomically tuned record of relative geomagnetic paleointensity from the western Philippine Sea, J. Geophys. Res. 108 (2003) 2059, doi:10.1029/2001JB001698.
[33] N. Thouveny, J. Carcaillet, E. Moreno, G. Leduc, D. Nérini, Geomagnetic moment variation and paleomagnetic excursions since 400 kyr BP: a stacked record from sedimentary sequences of the Portuguese margin, Earth Planet. Sci. Lett. 219 (2004) 377–396.
[34] U. Bleil, G. Gard, Chronology and correlation of Quaternary magnetostratigraphy and nannofossil biostratigraphy in Norwegian–Greenland Sea sediments, Geol. Rundsch. 78 (1989) 1173–1187.
[35] N.R. Nowaczyk, M. Baumann, Combined high-resolution magnetostratigraphy and nannofossil biostratigraphy for late Quaternary Artic Ocean sediments, Deep-Sea Res. 39 (1992) 567–601.
[36] N.R. Nowaczyk, T.W. Frederichs, A. Eisenhauer, G. Gard, Magnetostratigraphic data from late Quaternary sediments from the Yermak Plateau, Arctic Ocean: evidence for four geomagnetic polarity events within the last 170 ka of the Brunhes Chron, Geophys. J. Int. 117 (1994) 453–471.
[37] N.R. Nowaczyk, M. Antonow, High resolution magnetostratigraphy of four sediment cores from the Greenland Sea: I. Identification of the Mono Lake excursion, Laschamp and Biwa I/JAMAica geomagnetic polarity events, Geophys. J. Int. 131 (1997) 310–324.
[38] G. Wollin, D.B. Ericson, W.B.F. Ryan, J.H. Foster, Magnetism of the Earth and climate changes, Earth Planet. Sci. Lett. 12 (1971) 175–183.
[39] W.B.F. Ryan, J.D. Flood, Preliminary paleomagnetic measurements onsediments from the Ionian (Site 125) and Tyrrhenian (Site 132) basins of the Mediterranean Sea, in: W.B.F. Ryan, K.J. Hsu, et al., (Eds.), Initial Reports of the Deep Sea Drilling Project, vol. 13, U.S. Gov't Printing Office, Washington, DC, 1972, pp. 599–603.
[40] N. Kawai, K. Yaskawa, T. Nakajima, M. Torii, S. Horie, Oscillating geomagnetic field with a recurring reversal discovered from Lake Biwa, Proc. Jpn. Acad. 48 (1972) 186–190.
[41] N.R. Nowaczyk, J. Knies, Magnetostratigraphic results from the eastern Arctic Ocean: AMS ^{14}C ages and relative paleointensity data of the Mono Lake and Laschamp geomagnetic reversal excursions, Geophys. J. Int. 140 (2000) 185–197.
[42] J.C. Liddicoat, Mono Lake excursion in Mono Basin, California, and at Carson Sink and Pyramid Lake, Nevada, Geophys. J. Int. 108 (1992) 442–452.
[43] D.V. Kent, S.R. Hemming, B.D. Turrin, Laschamp excursion at Mono Lake? Earth Planet. Sci. Lett. 197 (2002) 151–164.
[44] L. Benson, J. Liddicoat, J. Smoot, A. Sarna-Wojcicki, R. Negrini, S. Lund, Age of the Mono lake excursion and associated tephra, Quat. Sci. Rev. 22 (2003) 135–140.
[45] G. Wagner, J. Beer, C. Laj, C. Kissel, J. Mazarik, R. Muscheler, H.-A. Synal, Chlorine-36 evidence for the Mono Lake Event in the Summit GRIP ice core, Earth Planet. Sci. Lett. 181 (2000) 1–6.
[46] C. Laj, C. Kissel, A.P. Roberts, Geomagnetic field behavior during the Iceland Basin and Laschamp geomagnetic excursions: a simple transitional field geometry? Geochem. Geophys. Geosyst. (in press).
[47] K.M. Creer, P.W. Readman, A.M. Jacobs, Paleomagnetic and paleontological dating of a Section at Gioa Tauro, Italy: identification of the Blake Event, Earth Planet. Sci. Lett. 50 (1980) 289–300.

[48] X. Fang, J. Li, R. Van der Voo, C. MacNiocaill, X. Dai, R.A. Kemp, E. Derbyshire, J. Cao, J. Wang, G. Wang, A record of the Blake Event during the last interglacial paleosol in the western loess plateau of China, Earth Planet. Sci. Lett. 146 (1997) 73–82.
[49] C.R. Denham, Blake polarity episode in two cores from the Greater Antilles outer ridge, Earth Planet. Sci. Lett. 29 (1976) 422–443.
[50] J.E.T. Channell, M.E. Raymo, Paleomagnetic record at ODP Site 980 (Feni Drift, Rockall) for the past 1.2 Myrs, Geochem. Geophys. Geosyst. (G^3) (2003), doi:10.1029/2002GC000440.
[51] Weeks, R.C. Laj, L. Endignoux, A. Mazaud, L. Labeyrie, A. Roberts, C. Kissel, E. Blanchard, Normalized NRM intensity during the last 240,000 years in piston cores from central North Atlantic Ocean: geomagnetic field intensity or environmental signal? Phys. Earth Planet. Int. 87 (1995) 213–229.
[52] T. Yamazaki, N. Ioka, Long-term secular variation of the geomagnetic field during the last 200 kyr recorded in sediment cores from the western equatorial Pacific, Earth Planet. Sci. Lett. 128 (1994) 527–544.
[53] J.S. Stoner, J.E.T. Channell, D.A. Hodell, C. Charles, A 580 kyr paleomagnetic record from the sub-Antarctic South Atlantic (ODP Site 1089), J. Geophys. Res. 108 (2003) 2244, doi:10.1029/2001JB001390.
[54] H. Oda, K. Nakamura, K. Ikehara, T. Nakano, M. Nishimura, O. Khlystov, Paleomagnetic record from Academician Ridge, Lake Baikal: a reversal excursion at the base of marine oxygen isotope stage 6, Earth Planet. Sci. Lett. 202 (2002) 117–132.
[55] J.C. Liddicoat, R.S. Coe, J.M. Glen, Record of the younger part of the Pringle Falls excursion at Long Valley, California, Geophys. J. Int. 135 (1998) 663–670.
[56] M. McWilliams, Global correlation of the 223 ka Pringle Falls Event, Int. Geol. Rev. 43 (2001) 191–195.
[57] B.S. Singer, B.R. Jicha, B.T. Kirby, X. Zhang, J.W. Geissman, E. Herrero-Brevera, An $^{40}Ar/^{39}Ar$ age for geomagnetic instability recorded at the Albuquerque Volcanoes and Pringle Falls, Oregon, Eos Trans. AGU 86 (52) (2005) (Fall Meeting Suppl., Abstract GP21A-0019).
[58] L. Clausen, Late Neogene and Quaternary sedimentation on the continental slope and upper rise offshore southeast Greenland: interplay of contour and turbidity processes, in: H.C. Larsen, A. D. Saunders, S.W. Wise Jr. (Eds.), Proc. ODP, Sci. Results, vol. 152, Ocean Drilling Program, College Station, TX, 1998, pp. 3–18.
[59] M. Elliot, L. Labeyrie, G. Bond, E. Cortijo, J.-L. Turon, N. Tisnerat, J.-C. Duplessy, Millennial-scale iceberg discharges in the Irminger Basin during the last glacial periods: relationship with the Heinrich events and environmental settings, Paleoceanography 13 (1998) 433–446.
[60] G. Bond, W. Showers, M. Elliot, M. Evans, R. Lotti, I. Hajdas, G. Bonani, S. Johnson, The North Atlantic's 1–2 kyr climate rhythm: relation to Heinrich Events, Dansgaard/Oeschger cycles and the Little Ice Age, in: Webb, et al., (Eds.), Mechanisms of Millennial-scale Global Climate Change, AGU Geophysical Monograph, vol. 112, 1999, pp. 35–58.
[61] C. Kissel, C. Laj, L. Labeyrie, T. Dokken, A. Voelker, D. Blamart, Rapid climatic variations during marine isotopic stage 3: magnetic analysis of sediments from Nordic seas and North Atlantic, Earth Planet. Sci. Lett. 171 (1999) 489–502.
[62] Shipboard Scientific Party, Site 919, in: H.C. Larsen, A.D. Saunders, P.D. Clift, et al., (Eds.), Proc. ODP, Initial Rep., vol. 152, Ocean Drilling Program, College Station, TX, 1994, pp. 257–277.
[63] K. Fukuma, Pliocene–Pleistocene magnetostratigraphy of sedimentary sequences from the Irminger Basin, in: H.C. Larsen, A. D. Saunders, S.W. Wise Jr. (Eds.), Proc. ODP, Sci. Results, vol. 152, 1998, pp. 265–269.
[64] B.P. Flower, Mid- to late Quaternary stable isotope stratigraphy and paleoceanography at Site 919 in the Irminger Basin, in: H.C. Larsen, A.D. Saunders, S.W. Wise Jr. (Eds.), Proc. ODP, Sci. Results, vol. 152, Ocean Drilling Program, College Station, TX, 1998, pp. 243–248.
[65] K. St. John, B.P. Flower, L. Krissek, Evolution of iceberg melting, biological productivity, and the record of Icelandic volcanism in the Irminger Basin since 630 ka, Mar. Geol. 212 (2004) 133–152.
[66] N.J. Shackleton, N.G. Pisias, Atmospheric carbon dioxide, orbital forcing, and climate, in: E.T. Sundquist, W.S. Broecker (Eds.), The Carbon Cycle and Atmospheric CO_2: Natural Variations Archean to Present, AGU Monograph, vol. 32, 1985, pp. 412–417.
[67] N.J. Shackleton, A. Berger, W.R. Peltier, An alternative astronomical calibration of the lower Pleistocene timescale based on ODP Site 677, Trans. R. Soc. Edinb. Earth Sci. 81 (1990) 251–261.
[68] N.J. Shackleton, The 100,000-year ice-age cycle identified and found to lag temperature, carbon dioxide, and orbital eccentricity, Science 289 (2000) 1897–1902.
[69] L.E. Lisiecki, M.E. Raymo, A Pliocene–Pleistocene stack of 57 globally distributed benthic $\delta^{18}O$ records, Paleoceanography 20 (2005) A1003, doi:10.1029/2004PA001071.
[70] Y. Guyodo, J.E.T. Channell, R. Thomas, Deconvolution of u-channel paleomagnetic data near geomagnetic reversals and short events, Geophys. Res. Lett. 29 (2002) 1845, doi:10.1029/2002GL014963.
[71] H. Oda, H. Shibuya, Deconvolution of long-core paleomagneic data of Ocean Drilling Program by Akaike's Bayesian criterion minimization, J. Geophys. Res. 101 (1996) 2815–2834.
[72] J.L. Kirschvink, The least squares lines and plane analysis of paleomagnetic data, Geophys. J. R. Astron. Soc. 62 (1980) 699–718.
[73] R. Thomas, Y. Guyodo, J.E.T. Channell, U-channel track for susceptibility measurements, Geochem. Geophys. Geosyst. (G^3) 1050 (2003), doi:10.1029/2002GC000454.
[74] J.W. King, S.K. Banerjee, J. Marvin, A new rock-magnetic approach to selecting sediments for geomagnetic paleointensity studies: application to paleointensity for the last 4000 years, J. Geophys. Res. 88 (1983) 5911–5921.
[75] L. Tauxe, Sedimentary records of relative paleointensity of the geomagnetic field: theory and practice, Rev. Geophys. 31 (1993) 319–354.
[76] W. Dansgaard, S.J. Johnson, H.B. Clausen, D. Dahl-Jensen, N. Gundestrup, C.U. Hammer, C.S. Hvidberg, J.P. Steffensen, A.E. Sveinbjornsdottir, J. Jouzel, G. Bond, Evidence for general instability of past climate from a 250 kyr ice core record, Nature 364 (1993) 218–220.
[77] P.M. Grootes, M. Stuiver, J.W.C. White, S.J. Johnsen, J. Jouzel, Comparison of oxygen isotope records from the GISP2 and GRIP Greenland ice cores, Nature 366 (1993) 552–554.
[78] R. Day, M. Fuller, V.A. Schmidt, Hysteresis properties of titanomagnetites: grain-size and compositional dependence, Phys. Earth Planet. Int. 13 (1977) 260–267.
[79] Y. Guyodo, J.-P. Valet, Global changes in intensity of the earth's magnetic field during the past 800 kyr, Nature 399 (1999) 249–252.
[80] K. Zhang, D. Gubbins, Is the geodynamo intrinsically unstable? Geophys. J. Int. 140 (2000) F1–F4.